IEEE Access
Multidisciplinary | Rapid Review | Open Access Journal

Received August 12, 2019, accepted August 24, 2019, date of publication September 12, 2019, date of current version October 1, 2019.

Digital Object Identifier 10.1109/ACCESS.2019.2940736

Development of Voxel Models Adjusted to ICRP Reference Children and Their Whole-Body Averaged SARs for Whole-Body Exposure to Electromagnetic Fields From 10 MHz to 6 GHz

TOMOAKI NAGAOKA, (Member, IEEE), AND SOICHI WATANABE, (Member, IEEE)
National Institute of Information and Communications Technology, Koganei 184-8795, Japan

Corresponding author: Tomoaki Nagaoka (nagaoka@nict.go.jp)

This work was supported by the Ministry of Internal Affairs and Communications, Japan.

ABSTRACT New child voxel models that are adjusted to the International Commission on Radiological Protection (ICRP)'s reference values (1-, 5- and 10-yr-old children) have been developed. The whole-body averaged specific absorption ratios (WBA-SARs) of these child voxel models were calculated for the whole-body exposure conditions with the E-polarization and H-polarization plane wave incidence from 10 MHz to 6 GHz. The WBA-SARs are 40% to 60% higher for the child voxel models than for adult voxel models adjusted to the ICRP's reference values (NORMAN and NAOMI). The WBA-SARs of the child voxel models exceed the basic restriction by at most 20% or 0.08 W/kg for the general environment when the incident power density is set to the reference level at each frequency of the ICNIRP's RF safety guidelines.

INDEX TERMS EMF dosimetry, specific absorption rate (SAR), children.

I. INTRODUCTION

Human body exposure to an excessively high strength radio-frequency (RF) electromagnetic field (EMF) can cause thermal effects. The whole-body averaged specific absorption rate (WBA-SAR) has been used as a measure of the thermal effect due to whole-body heating caused by RF EMF. The SAR is defined as the power absorbed in a unit mass of a human body and the WBA-SAR is derived by dividing the total power absorbed in a whole human body by the whole-body mass.

The International Commission on Non-Ionizing Radiation and Protection (ICNIRP) has therefore set the basic restrictions in terms of the WBA-SAR in its RF safety guidelines [1].

Because it is difficult to directly evaluate the WBA-SAR, other guideline levels or reference levels have also been introduced in the ICNIRP guidelines. The reference levels are the incident electric and magnetic fields or power density that correspond to the basic restrictions of the WBA-SAR under the whole-body exposure condition as the worst condition. Numerical dosimetry using voxel human models has been playing an important role in determining the reference levels [2].

One of the most important findings from the numerical dosimetry using voxel human models is that the current reference levels do not always limit the WBA-SAR to within its basic restrictions when people of small stature or children are exposed to RF EMF [3]–[13]. Concerning this issue, the ICNIRP has released a statement that the WBA-SAR of children can exceed about 40% of the basic restrictions even if the incident RF EMF is equal to or lower than the reference level, and such excess is significantly lower than the reduction factor considered in their guidelines, i.e., 5000% [14]. However, a recent revision of the safety standard issued by Health Canada has changed the incident EMF limits while taking into consideration the increase in the WBA-SAR of children [15].

To improve the RF safety guidelines for protecting children, it is clearly important to investigate the detailed characteristics of the WBA-SAR of children. Most child voxel models, however, have been developed on the basis of adult

The associate editor coordinating the review of this manuscript and approving it for publication was Mohamed Kheir.

voxel models by scaling to fit with the height and weight of children [3]–[7]. These models, however, have fatal discrepancies with actual children with regard to the body shape and internal-tissue structure. To overcome these discrepancies, some models have been adjusted to the body shape of children [8], [9], [12]. A few models have recently been developed on the basis of the magnetic resonance imaging (MRI) data of actual children [16], [17]. Although MRI-based voxel models have better accuracy in terms of the body shape and internal-tissue structure, they have been highly specific to the individual child from whom the MRI scan was taken. Thus, it is difficult to extract general characteristics from calculations using the MRI-based voxel models. Therefore, to discuss the typical characteristics of the WBA-SAR of children, reference child models are necessary.

For ionizing radiation protection, the International Commission on Radiological Protection (ICRP) has issued the reference values of standard human bodies [18], in which the reference values of not only height and whole-body weight but also internal tissue weights are listed. Previously, adult male and female voxel models adjusted to the ICRP's reference values were developed and used for evaluating the WBA-SAR [3], [5]. Child voxel models adjusted to the ICRP's reference values have not been developed. Therefore, in this study, we have developed child voxel models adjusted to the ICRP's reference values and investigated the WBA-SAR characteristics of these models. On the basis of the WBA-SAR characteristics derived from the calculations using these reference models, we have also discussed the increase in the WBA-SAR of children and the validity of the reference levels of the RF safety guidelines.

II. METHODS AND MODELS

A. CALCULATION METHOD

The finite-difference time-domain (FDTD) method [19] was used for the calculation of the WBA-SAR of the child voxel models exposed to a plane wave ranging from 10 MHz to 6 GHz using an in-house multi-GPU-based FDTD solver. The validity of the SAR calculation using our solver has been verified by an intercomparison [20]. The FDTD lattice size was 2 mm below 2 GHz, 1 mm from 2 GHz to 5 GHz and 0.5 mm at 6 GHz. The lattice size for each frequency was optimized on the basis of previous literature in which the relationship between the lattice size and the WBA-SAR was examined [13]. The split perfectly matched layer (SPML) boundary conditions [19] were used to truncate the calculation region without any significant reflection. The 8-layer SPML boundaries are located at least 18 cells from the voxel models.

The details of the child voxel models are described in the following subsection. The electrical properties of the voxel models were taken from a previous report [21].

The whole-body exposure conditions were considered in the calculations conducted in this paper. Two polarization conditions, i.e., E- and H-polarizations, were considered. The incident direction was from the front to the back.

The WBA-SAR is defined using the following equation:

$$\mathrm{WBA-SAR} = \int_V \sigma E^2 \, dV \Big/ \int_V \rho dV \,[\mathrm{W/kg}], \qquad (1)$$

where σ is the conductivity of the tissue (S/m), ρ is the density of the tissue (kg/m^3), E is the root mean square of the internal electric field (V/m), and V is the volume of the whole body. The WBA-SARs in most figures in this paper were then normalized as the incident power density was 1 W/m^2.

B. CHILD VOXEL MODELS ADJUSTED TO ICRP'S REFERENCE VALUES

ICRP has reported the reference values of four children, i.e., 1-, 5-, 10- and 15-yr-old children [18]. Because the body shape of the 15-yr-old child is similar to those of adults, we have therefore developed 1-, 5- and 10-yr-old child voxel models as described below.

It is difficult to acquire whole-body MR image data with the fine resolution necessary for generating child models having anatomical structures that match the ICRP's reference values owing to the difficulties in recruiting children and ethical problems. Therefore, we applied the existing data and a deformation technique to voxel models to develop the child models adjusted to the ICPR's reference values. For the 1-yr-old child voxel model, we first obtained the body-shape data from the poor quality MRI data of a 1-yr-old child. Then, we deformed a 3-yr-old child voxel model, which was previously developed on the basis of the MRI data of a 3-yr-old child, to fit with the body shape of the 1-yr-old child using the volume morphing technique [22]. For the 10-yr-old child voxel model, we also obtained the 3D laser scan data of a 10-yr-old child. Then, we deformed a 7-yr-old child voxel model, which was previously developed on the basis of the MRI data of a 7-yr-old child, to fit with the body shape of the 10-yr-old child using the same technique. For the 5-yr-old child voxel model, we used the same 5-yr-old child voxel model, which was previously developed on the basis of a 5-yr-old child.

In the second step, we then adjusted the height, weight and internal-tissue masses to their reference values in the ICRP publication [18] by the volume morphing technique [22] and manual editing of the voxels. Finally, these voxel models were diagnosed and corrected by medical experts.

The developed child voxel models are shown in Fig. 1. These models are composed of voxels of $2\times2\times2$ mm^3. These models have realistic body shapes corresponding to their ages and it has been confirmed by medical doctors that they have no unnatural anatomical structures. The representative parameters of the child voxel models as well as the ICRP's reference values are listed in Table 1. The differences from the ICRP's reference values are within 1% for the heights and weights of these models, and within 10% for the main internal-tissue masses.

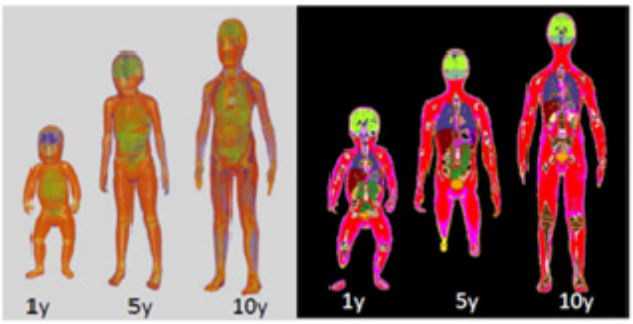

FIGURE 1. Child voxel models adjusted to the ICRP's reference values for 1-, 5- and 10-yr-old children. The left picture shows the transparent outer shapes of the child voxel models. The right picture shows the internal structures of the child voxel models.

TABLE 1. Compilation of the body dimensions and weights of the developed child voxel models and the corresponding ICRP reference values [18].

		Developed models	ICRP's reference values	Differences
1yr	Height	76.0 [cm]	76.0 [cm]	0 [%]
	Weight	10.0 [kg]	10.0 [kg]	0 [%]
	Brain mass	892 [g]	950[g]	6 [%]
	Heart mass	54 [g]	50 [g]	8 [%]
	Liver mass	301 [g]	330 [g]	9 [%]
	Lung mass	150 [g]	150 [g]	0 [%]
	Fat mass	2166 [g]	2300 [g]	6 [%]
	Muscle mass	2050 [g]	1900 [g]	8 [%]
	Skeleton mass	1214 [g]	1170 [g]	4 [%]
5yr	Height	109.0 [cm]	109.0 [cm]	0 [%]
	Weight	18.8 [kg]	19.0 [kg]	1 [%]
	Brain mass	1319 [g]	1310 [g]	1 [%]
	Heart mass	85 [g]	85 [g]	0 [%]
	Liver mass	552 [g]	570 [g]	3 [%]
	Lung mass	301 [g]	300 [g]	0 [%]
	Fat mass	3631 [g]	3600 [g]	1 [%]
	Muscle mass	5941 [g]	5600 [g]	6 [%]
	Skeleton mass	2537 [g]	2430 [g]	4 [%]
10yr	Height	138.0 [cm]	138.0 [cm]	0 [%]
	Weight	31.9 [kg]	32.0 [kg]	0 [%]
	Brain mass	1405 [g]	1400 [g]	0 [%]
	Heart mass	146 [g]	140 [g]	4 [%]
	Liver mass	800 [g]	830 [g]	4 [%]
	Lung mass	505 [g]	500 [g]	1 [%]
	Fat mass	6293 [g]	6000 [g]	5 [%]
	Muscle mass	11935 [g]	11000[g]	8 [%]
	Skeleton mass	4711 [g]	4500 [g]	5 [%]

III. RESULTS

Table 2 lists the calculated results of the WBA-SARs of the child voxel models. Figure 2 shows the frequency characteristics of the WBA-SARs of the child voxel models. The WBA-SARs of the adult male and female adjusted to the ICRP's reference models [18] are also shown in the same figure.

The whole-body resonance appears for the cases under the E-polarization conditions. The resonant frequency depends on the height, i.e., 150, 100 and 90 MHz for the 1-, 5- and 10-yr-old child voxel models, respectively. However, the WBA-SARs at the resonant frequency are similar among these child voxel models (±1.5%).

TABLE 2. Calculated results of the WBA-SARs (W kg^{-1}) of the child voxel models adjusted to the 1-, 5- and 10-yr-old child ICRP reference values. The incident power density is 1 W/m^2.

	E-polarization			H-polarization		
F [MHz]	1y	5y	10y	1y	5y	10y
10	2.42E-04	5.45E-04	6.21E-04	5.28E-05	1.12E-04	1.20E-04
20	1.23E-03	2.39E-03	2.53E-03	1.76E-04	3.66E-04	3.29E-04
30	2.36E-03	4.05E-03	4.95E-03	3.60E-04	6.77E-04	6.57E-04
40	3.42E-03	7.40E-03	1.07E-02	5.70E-04	1.00E-03	1.02E-03
50	5.14E-03	1.24E-02	1.76E-02	7.85E-04	1.32E-03	1.38E-03
60	7.70E-03	1.85E-02	2.53E-02	1.03E-03	1.65E-03	1.72E-03
70	1.09E-02	2.49E-02	3.27E-02	1.30E-03	2.01E-03	2.10E-03
80	1.45E-02	3.14E-02	3.91E-02	1.57E-03	2.39E-03	2.50E-03
90	1.84E-02	3.79E-02	4.20E-02	1.89E-03	2.81E-03	2.95E-03
100	2.24E-02	4.31E-02	3.88E-02	2.23E-03	3.26E-03	3.44E-03
120	3.12E-02	4.30E-02	2.60E-02	3.04E-03	4.30E-03	4.43E-03
150	4.16E-02	2.84E-02	1.61E-02	4.63E-03	5.99E-03	5.43E-03
180	3.74E-02	2.00E-02	1.33E-02	6.83E-03	7.32E-03	5.67E-03
200	3.07E-02	1.78E-02	1.30E-02	8.54E-03	7.72E-03	5.68E-03
300	1.77E-02	1.54E-02	1.11E-02	1.17E-02	7.51E-03	5.80E-03
400	1.60E-02	1.31E-02	9.38E-03	1.02E-02	7.53E-03	6.09E-03
500	1.53E-02	1.22E-02	9.75E-03	1.00E-02	8.04E-03	6.77E-03
600	1.40E-02	1.31E-02	9.80E-03	1.02E-02	8.99E-03	7.90E-03
700	1.38E-02	1.26E-02	9.78E-03	1.06E-02	9.98E-03	8.01E-03
800	1.46E-02	1.21E-02	9.55E-03	1.15E-02	1.01E-02	8.03E-03
900	1.51E-02	1.19E-02	9.46E-03	1.21E-02	9.82E-03	8.27E-03
1000	1.46E-02	1.17E-02	9.50E-03	1.21E-02	9.70E-03	8.37E-03
2000	8.50E-03	9.31E-03	7.79E-03	8.68E-03	8.83E-03	7.39E-03
3000	7.40E-03	8.57E-03	6.00E-03	1.01E-02	8.43E-03	5.98E-03
4000	7.66E-03	8.08E-03	5.37E-03	9.85E-03	8.71E-03	5.94E-03
5000	8.22E-03	7.76E-03	5.83E-03	1.04E-02	8.67E-03	6.62E-03
6000	8.78E-03	7.31E-03	5.97E-03	1.11E-02	8.54E-03	7.02E-03

Because no resonance appears for the cases under the H-polarization conditions, the differences in the WBA-SAR between the E- and H-polarizations are significantly large, e.g., 92% for the 5-yr-old child voxel model at the resonant frequency, whereas the dependences on the age are relatively small, e.g., 35% and 25% of the relative variation in the WBA-SARs between the 1-, 5- and 10-yr-old child voxel models for the cases of E- and H-polarizations, respectively, at 100 MHz.

Above the resonant frequency or GHz region, the WBA-SAR tends to increase with decreasing age. This tendency is especially clear for the cases of H-polarization, where the WBA-SARs of the 1-yr-old child model increase by 17% and 58% from those of the 10-yr-old child model at 2 and 6 GHz, respectively. It is also shown that the WBA-SARs for the cases of H-polarization are generally higher than those of E-polarization, e.g., 26% increases for the 1-yr-old child model at 6 GHz (11.1 and 8.78 mW/kg for the H- and E-polarizations, respectively).

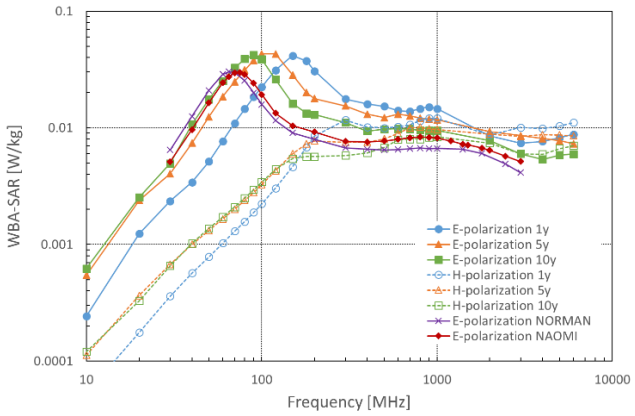

FIGURE 2. Frequency characteristics of the WBA-SAR of the child voxel models adjusted to the 1-, 5- and 10-yr-old child ICRP reference values. The incident power density is 1 W/m^2. The WBA-SARs of the adult male and female voxel models adjusted to the ICRP's reference values are also plotted [4], [5].

The variations of the WBA-SARs due to the child ages (1, 5 and 10 yr) are then statistically analyzed below. The variations due to the child ages are averaged at the frequencies listed in Table 2 from 10 MHz to 6 GHz; the averaged values of the variations are 29% and 19% for the E- and H-polarizations, respectively. The maximum values of the variations are 59% and 40% for the E- and H-polarizations, respectively.

The WBA-SARs of the child voxel models are also compared with those of the adult voxel models, i.e., NORMAN and NAOMI, which represent the adult male and female voxel models adjusted to the ICRP's reference values, respectively [3], [5]. The WBA-SARs of the child voxel models are higher than those of the adult voxel models (relative increases of 42% and 58%, respectively, at the whole-body resonant frequency). At the resonant frequency, the relative difference in the WBA-SARs among the three child voxel models is 2% and similar to the relative difference in the WBA-SARs between the adult male and female voxel models, i.e., 1%. This suggests that gender is not a dominant factor of the WBA-SAR around the whole-body resonant frequency region.

The differences due to the gender of the adult voxel models increase at higher frequencies, e.g., an 11% relative difference at 3 GHz, compared with those at the whole-body resonant frequency region. The differences due to age also become larger than those in the whole-body resonant frequency region, e.g., 18% of the relative difference at 3 GHz.

TABLE 3. Comparison of the specifications of the child voxel models between this study and previous studies.

	ICRP			Body shape	Base data	Ref. data
	Height[a]	Weight[a]	Internal tissues[b]			
1-yr-old child model						
NICT (this study)	0%	0%	Adjusted	Real	3-yr-old JP child model	MRI of a 1-yr-old child
ETRI [12]	-2%	-3%	No	No	7-yr-old KR child model	
HPA [3]	-1%	0%	No	No	Adult male model (NORMAN)	
HPA [5]	0%	0%	No	No	Adult female model (NAOMI)	
UF [13]	-7%	-13%	No	Real	CT of a 9-month-old patient	
5-yr-old child model						
NICT (this study)	0%	1%	Adjusted	Real	5-yr-old JP child model	
ETRI [12]	-1%	-2%	No	No	7-yr-old KR child model	
HPA [3]	-1%	5%	No	No	Adult male model (NORMAN)	
HPA [5]	0.%	0%	No	No	Adult female model (NAOMI)	
VF (Thelonious) [16]	-7%	-13%	No	Real	6-yr-old GE child model	
10-yr-old child model						
NICT (this study)	0%	0%	Adjusted	Real	7-yr-old JP child model	3D scan of a 10-yr-old child
HPA(1) [3]	0%	3%	No	No	Adult male model (NORMAN)	
HPA [5]	0%	0%	No	No	Adult female model (NAOMI)	
VF (Billie) [16]	5.8%	13%	No	Real	11-yr-old GE child model	

[a]Percentage difference from ICRP's reference value.
[b]Masses of internal tissues of the model relative to the ICRP's reference values.

IV. DISCUSSION

A. COMPARISON WITH OTHER CHILD MODELS

Table 3 compares the specifications of the child voxel models between this study and previous studies. As well as the child voxel models developed in this study, the height and body weight of the other child voxel models developed by scaling other age (mostly adult) voxel models are adjusted to the ICRP's reference values. However, the body shapes of some models are not properly adjusted to real children, and the internal-tissue structures of these models are also not adjusted. If homogeneous scaling is applied to an adult voxel model to develop a child voxel model, for example,

the body shape and internal-tissue structure can significantly differ from those of actual children.

Some child voxel models were developed on the basis of X-ray computer tomography (CT) and MRI data of actual children [13], [16], [17]. The body shape and internal-tissue structure are highly realistic compared with those of other scaled child voxel models. The body shape and internal-tissue structure of the child voxel models previously developed on the basis of the X-ray CT and MRI data of actual children are, however, not adjusted to the ICRP's reference values [18].

Thus, it is clear that only the child voxel models developed in this study are adjusted to the ICRP's reference values with regard to not only height and body weight but also body shape and internal-tissue structure, which are called the ICRP child voxel models hereafter.

Figure 3 compares the WBA-SARs between the ICRP child voxel models and the other child voxel models [4], [5]. The child voxel models developed by Dimbylow [3], [5] were homogeneously scaled from the adult male and female voxel models called NORMAN and NAOMI, respectively, to fit with the height and whole-body weight of the ICRP's reference values.

At the whole-body resonant frequencies, the differences in the WBA-SARs between the ICRP child voxel models and the homogeneously scaled child voxel models are at most 15%. Note that the frequency resolution was insufficient to identify the whole-body resonant frequency, which may cause an additional uncertainty in this comparison. The WBA-SARs of the child voxel models scaled from the adult female model or NAOMI are lower than those of the other child voxel models, e.g., 14% lower than that of the ICRP 10-yr-old child voxel model, which suggests that gender can affect the whole-body resonance in the case of child exposure, whereas no such effect was found in the case of adult exposure (see Fig. 1).

Around the GHz region, the differences in the WBA-SARs between the ICRP child voxel models and the homogeneously scaled child voxel models significantly increase, i.e., up to 42% compared with those in the resonant frequency region. The frequency tendency, however, is slightly different between these models; the WBA-SARs of the homogeneously scaled child voxel models are higher than those of the ICRP child voxel models at 1 GHz, whereas the opposite relationship is shown at 3 GHz.

It is also interesting to note that the WBA-SARs of the child voxel models scaled from the adult female voxel model or NAOMI are closer to those of the ICRP's child voxel models than those of the child voxel models scaled from the adult male voxel model or NORMAN, e.g., the differences in the WBA-SARs between the ICRP child voxel models and the child voxel models scaled from NAOMI range from −7% to 8% with an average of 1% at 1 GHz whereas those between the ICRP child voxel models and the child voxel models scaled from NORMAN range from −22% to −10% with an average of −16%, which shows the opposite tendency

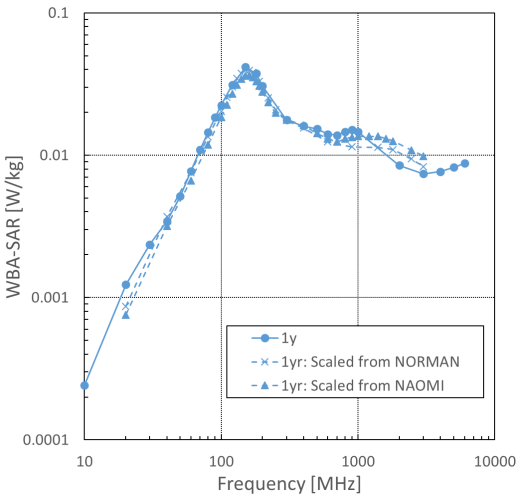

(a) WBA-SARs of the 1-yr-old child voxel models

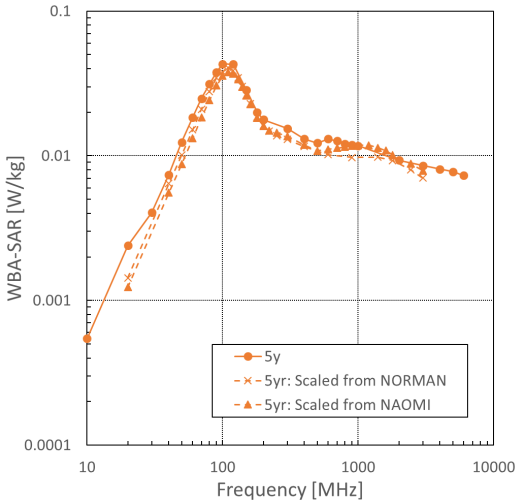

(b) WBA-SARs of the 5-yr-old child voxel models

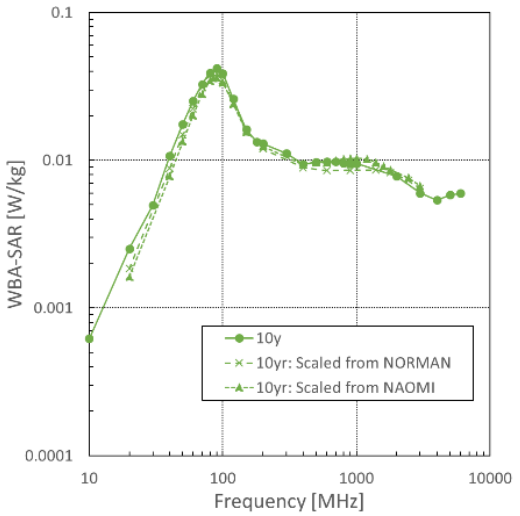

(c) WBA-SARs of the 10-yr-old child voxel models

FIGURE 3. Comparison of the WBA-SARs between the child voxel models adjusted to the ICRP's child reference values in this study and the other child voxel models developed in previous studies [4], [5].

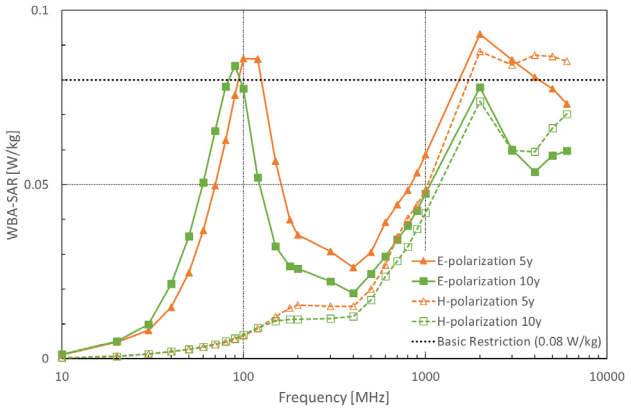

FIGURE 4. Frequency characteristics of the WBA-SARs of the ICRP child voxel models when the incident power density is set to the reference level at each frequency.

to the case of the whole-body resonant frequency region. Because the body shape of the adult female voxel model is closer to a child's body shape than that of the adult male voxel model, the voxel child models scaled from the adult female model may be more appropriate for this frequency region where part-body resonant phenomena may contribute to the WBA-SARs.

B. RELATIONSHIP WITH THE BASIC RESTRICTION OF THE WHOLE-BODY AVERAGED SAR

To discuss the validity of the current reference levels of the RF safety guidelines, the WBA-SARs of the ICRP child voxel models when the incident power density is set to the reference level at each frequency are shown in Fig. 4.

Around the whole-body resonant frequency of 100 MHz and 2 GHz, some of the WBA-SARs of the ICRP child voxel models exceed the basic restriction of the ICNIRP guidelines [1]. The excesses of the WBA-SARs are within 16% and 5% for the 5- and 10-yr-old child voxel models, respectively, which are significantly lower than the excess of the WBA-SARs of children or 40% as reported previously [14]. In this study, we estimated the WBA-SARs in only isolate conditions. It is known that the WBA-SARs under grounded conditions are not significantly different from those under isolated conditions, whereas the whole-body resonant frequencies shift to about half the frequencies under isolated conditions, and the WBA-SARs under grounded conditions are also rather equivalent to those under isolated conditions in the GHz band [3], [5]. Therefore, the results strongly indicate that the relationship with the basic restriction of WBA-SAR under grounded conditions shows a similar tendency to that under isolated conditions in the GHz region.

We must also consider the uncertainty included in our calculations and other factors that can affect the discussion on the validity of the reference levels of the RF safety guidelines. The main uncertainty factors included in our calculations are the uncertainty of the electrical properties and the calculation algorithm to evaluate the whole-body averaged SAR from the FDTD calculation results. The impact of the uncertainty of the electrical properties on the whole-body averaged SARs was investigated previously, and it was reported that the uncertainty of the WBA-SARs due to the dielectric properties is at most 11% [20]. The calculation algorithm to evaluate the whole-body averaged SAR is also another important factor, especially at higher frequencies. Dimbylow et al. reported that the use of a different calculation algorithm results in 18% of the difference in the WBA-SAR [20]. Although there are many uncertainty factors, their impact on the WBA-SAR is less significant than the above uncertainty factors, typically within a few percent [16].

Two of the factors that are not investigated in this paper are the incident angle and polarization; only two polarizations, E and H, and one direction, front to back, were considered in this study. Other conditions regarding the polarization and direction can cause higher WBA-SARs than those evaluated in this study. Note that these factors were investigated previously, and it was reported that the conditions assumed in this study generally result in the highest WBA-SARs [23]–[25].

Note also that the excess of the WBA-SARs of the 1-yr-old child voxel model reaches 39%, which is not shown in Fig. 4. We removed the data of the 1-yr-old child voxel model because it is unrealistic that a 1-yr-old child will continue to stand alone for over 6 minutes, the averaging time for the basic restriction of the WBA-SAR. The excess of the WBA-SARs appears in special cases where the coupling of the human body with the incident EMF becomes maximum. If the posture and direction change, the WBA-SARs considerably decrease from the maximum value under the best coupling condition. The WBA-SARs around the whole-body resonance frequency and 2 GHz in the cases of K-polarization, where the long axis of the model is parallel to the propagating direction of the plane wave (k-direction), are lower than 10% and 50% of those of E-and H-polarizations, respectively. A similar tendency was also reported elsewhere [2]. Recently, Hirata et al. have reported that the increase in the body-core temperature of children is generally lower than that of adults under the same WBA-SAR condition because the ratio of the surface area to the volume of the body is larger for children than for adults, which results in the effective cooling of children by external air [23]. This finding also weakens the significance of the excess of the WBA-SARs for children.

Consequently, the excess of the WBA-SARs for children (a few ten percent) is comparable with or less than the effects due to other factors, e.g., individual differences, environmental temperature, and relative polarization. This is consistent with the recent view of the ICNIRP [26] as well as its previous view [14] that the excess of the WBA-SARs for children is not significant, and there is no reason to modify the current reference levels.

V. CONCLUSON

The excess of the WBA-SARs for children was reported previously. However, the child voxel models used in the previous

studies were not standardized. Therefore, new child voxel models have been developed in this study.

The child voxel models were based on the other child voxel models that were based on the MRI data of children (3-, 5- and 7-yr-old children). The original child voxel models were modified to fit the outer shape of the child with the target age or 1-, 5- and 10-yr-old children. The body dimensions and whole-body weight and tissue weights were then adjusted to the ICRP's reference values [18].

The WBA-SARs of the developed child voxel models were calculated and compared with those of the adult voxel models adjusted to the ICRP's reference values. The variations in the WBA-SARs between the developed ICRP child voxel models were generally within 20% to 30%, whereas the WBA-SARs were higher for the child voxel models than for the adult voxel models (40% to 60%).

The WBA-SARs of the developed child voxel models were also compared with those of the other child voxel models, most of which were homogeneously scaled from the adult voxel models. The differences were up to 40%, similar to the level of variation due to the different ages as described above.

Finally, the excess of the WBA-SARs for children against the basic restrictions of the RF safety guidelines was discussed. The excess of the WBA-SAR was at most 20% for the developed 5- and 10-yr-old child voxel models adjusted to the ICRP's reference values, which is lower than the reported value or 40% in a previous review [14]. Although greater excess was shown for the 1-yr-old child voxel model, it is unrealistic to expect a 1-year-old child to continue standing alone for over 6 minutes. The findings of this study are useful for discussing the validity of the reference levels of the RF safety guidelines, such as those of the ICNIRP, which are currently being revised.

ACKNOWLEDGMENT

The child voxel models developed in this study will be available on NICT's webpage (http://emc.nict.go.jp) in the near future.

REFERENCES

[1] The International Commission on Non-Ionizing Radiation Protection, "Guidelines for limiting exposure to time-varying electric, magnetic, and electromagnetic fields (up to 300 GHz)," *Health Phys.*, vol. 74, no. 4, pp. 494–522, Apr. 1998.

[2] *Exposure to High Frequency Electromagnetic Fields, Biological Effects and Health Consequences (100 kHz-300 GHz)—Review of the Scientific Evidence and Health Consequences*, ICNIRP, Munich, Germany, 2009.

[3] P. J. Dimbylow, "FDTD calculations of the whole-body averaged SAR in an anatomically realistic voxel model of the human body from 1 MHz to 1 GHz," *Phys. Med. Biol.*, vol. 42, no. 3, pp. 479–490, 1997.

[4] P. J. Dimbylow, "Fine resolution calculations of SAR in the human body for frequencies up to 3 GHz," *Phys. Med. Biol.*, vol. 47, no. 16, pp. 2835–2846, 2002.

[5] P. J. Dimbylow, "Resonance behaviour of whole-body averaged specific energy absorption rate (SAR) in the female voxel model, NAOMI," *Phys. Med. Biol.*, vol. 50, pp. 4053–4063, Sep. 2005.

[6] J. Wang, O. Fujiwara, S. Kodera, and S. Watanabe, "FDTD calculation of whole-body average SAR in adult and child models for frequencies from 30 MHz to 3 GHz," *Phys. Med. Biol.*, vol. 51, no. 17, pp. 4119–4127, 2006.

[7] E. Piuzzi, P. Bernardi, M. Cavagnaro, S. Pisa, and J. C. Lin, "Analysis of adult and child exposure to uniform plane waves at mobile communication systems frequencies (900 MHz–3 GHz)," *IEEE Trans. Electromagn. Compat.*, vol. 58, no. 1, pp. 38–47, Feb. 2011.

[8] T. Nagaoka, E. Kunieda, and S. Watanabe, "Proportion-corrected scaled voxel models for Japanese children and their application to the numerical dosimetry of specific absorption rate for frequencies from 30 MHz to 3 GHz," *Phys. Med. Biol.*, vol. 53, pp. 6695–6711, Dec. 2008.

[9] E. Conil, A. Hadjem, F. Lacroux, M. F. Wong, and J. Wiart, "Variability analysis of SAR from 20 MHz to 2.4 GHz for different adult and child models using finite-difference time-domain," *Phys. Med. Biol.*, vol. 53, no. 6, pp. 1511–1525, 2008.

[10] A. Hirata, Y. Nagaya, F. Osamu, T. Nagaoka, and S. Watanabe, "Correlation between absorption cross section and body surface area of human for far-field exposure at GHz bands," in *Proc. IEEE Int. Symp. Electromagn. Compat.*, Honolulu, HI, USA, Jul. 2007, pp. 1–4.

[11] T. Nagaoka and S. Watanabe, "Estimation of variability of specific absorption rate with physical description of children exposed to electromagnetic field in the VHF band," in *Proc. IEEE Int. Conf. (EMBS)*, Minneapolis, MN, USA, Sep. 2009, pp. 942–945.

[12] A. K. Lee and H. D. Choi, "Determining the influence of Korean population variation on whole-body average SAR," *Phys. Med. Biol.*, vol. 57, pp. 2709–2725, May 2012.

[13] P. Dimbylow and W. Bolch, "Whole-body-averaged SAR from 50 MHz to 4 GHz in the University of Florida child voxel phantoms," *Phys. Med. Biol.*, vol. 52, no. 22, pp. 6639–6649, 2007.

[14] ICNIRP, "ICNIRP statement on the guidelines for limiting exposure to time-varying electric, magnetic, and electromagnetic fields (up to 300 GHz)," *Health Phys.*, vol. 97, no. 3, pp. 257–258, Sep. 2009.

[15] *Safety Code 6*, Health Canada, Ottawa, ON, Canada, 2015.

[16] A. Christ, W. Kainz, E. G. Hahn, K. Honegger, M. Zefferer, E. Neufeld, W. Rascher, R. Janka, W. Bautz, J. Chen, B. Kiefer, P. Schmitt, H.-P. Hollenbach, J. Shen, M. Oberle, D. Szczerba, A. Kam, J. W. Guag, and N. Kuster, "The virtual family—Development of surface-based anatomical models of two adults and two children for dosimetric simulations," *Phys. Med. Biol.*, vol. 55, no. 2, pp. N23–N38, 2010.

[17] T. Nagaoka and S. Watanabe, "Japanese voxel-based computational models and their applications for electromagnetic dosimetry," in *Proc. URSI GA*, Aug. 2011, pp. 1–4.

[18] *ICRP Publication 89: Basic Anatomical and Physiological Data for Use in Radiological Protection Reference Values*, ICRP, Ottawa, ON, Canada, 2002.

[19] A. Taflove and S. C. Hagness, *Computational Electrodynamics: The Finite-Difference Time-Domain Method*, 3rd ed. London, U.K.: Artech House, 2005.

[20] P. J. Dimbylow, A. Hirata, and T. Nagaoka, "Intercomparison of whole-body averaged SAR in European and Japanese voxel phantoms," *Phys. Med. Biol.*, vol. 53, pp. 5883–5897, Oct. 2008.

[21] C. Gabriel, "Compilation of the dielectric properties of body tissues at RF and microwave frequencies," Armstrong Lab., Brooks Air Force Base, San Antonio, TX, USA, Tech. Rep. AL/OE-TR-1996-0037, 1996.

[22] T. Nagaoka and S. Watanabe, "Voxel-based variable posture models of human anatomy," *Proc. IEEE*, vol. 97, no. 12, pp. 2015–2025, Dec. 2009.

[23] A. Hirata, N. Ito, and O. Fujiwara, "Influence of electromagnetic polarization on the whole-body averaged SAR in children for plane-wave exposures," *Phys. Med. Biol.*, vol. 54, pp. N59–N65, Feb. 2009.

[24] S. Kühn, W. Jennings, A. Christ, and N. Kuster, "Assessment of induced radio-frequency electromagnetic fields in various anatomical human body models," *Phys. Med. Biol.*, vol. 54, pp. 875–890, Feb. 2009.

[25] E. Conil, A. Hadjem, A. Gati, M.-F. Wong, and J. Wiart, "Influence of plane-wave incidence angle on whole body and local exposure at 2100 MHz," *IEEE Trans. Electromagn. Compat.*, vol. 53, no. 1, pp. 48–52, Feb. 2011.

[26] *Draft ICNRP Guidelines, Guidelines for Limiting Exposure to Time-Varying Electric, Magnetic and Electromagnetic Fields (100 kHz to 300 GHz)*, ICNIRP, Munich, Germany, 2018.

TOMOAKI NAGAOKA (M'06) received the Ph.D. degree in medical science from Kitasato University, Tokyo, Japan, in 2004. He is currently a Senior Researcher with the Electromagnetic Compatibility Laboratory, Applied Electromagnetic Research Institute, National Institute of Information and Communications Technology, Tokyo. His main research interests include biomedical electromagnetic compatibility and medical image analysis. He is a member of the IEEE Microwave Theory and Techniques Society and the Institute of Electronics, Information and Communication Engineers, Japan. He received several awards, including the 2004 Best Paper Award in Physics, Medicine, and Biology, the 2007 Young Researcher Award from the IEICE, the 2008 International Scientific Radio Union Young Scientist Award, the 2011 Outstanding Paper Award from the IEEE AFRICON, and the 2011 Best Paper Award from ISABEL'11.

SOICHI WATANABE (S'93–M'96) received the B.E., M.E., and D.E. degrees in electrical engineering from Tokyo Metropolitan University, Tokyo, Japan, in 1991, 1993, and 1996, respectively. He is currently with the National Institute of Information and Communications Technology, Tokyo. His main research interest includes biomedical electromagnetic compatibility. He was a member of the Standing Committee III on Physics and Engineering of International Commission on Non-Ionizing Radiation Protection, from 2004 to 2012, and the Main Commission of ICNIRP, since 2012. He is a member of the Institute of Electronics, Information and Communication Engineers, the Institute of Electrical Engineers, Japan, and the Bioelectromagnetics Society. He received the 1996 Young Scientist Award from the International Scientific Radio Union, the 1997 Best Paper Award from IEICE, and the 2004 Best Paper Award (The Roberts Prize) of Physics in Medicine and Biology.